International Journal of Robotics and Control Systems
Vol. 5, No. 1, 2025, pp. 159-178
ISSN 2775-2658
http://pubs2.ascee.org/index.php/ijrcs

Hybrid PI-MPC Control System for a Four-Phase Interleaved Boost Converter: Performance Evaluation in Reducing Current Ripple in Electric Car Battery Charging

Beauty Anggraheny Ikawanty [a,1,*], Hari Kurnia Safitri [a,2], Mila Fauziyah [a,3], Bambang Irawan [b,4], Taufik [c,5], Anindya Dwi Risdhayanti [a,6]

[a] Department of Electronics Engineering, Faculty of Electrical Engineering, Politeknik Negeri Malang, Indonesia
[b] Department of Mechanical Engineering, Faculty of Mechanical Engineering, Politeknik Negeri Malang, Indonesia
[c] Departement of Electrical Engineering, California Polytechnic State University, San Luis Obispo, California, USA
[1] beauty.anggraheny@polinema.ac.id; [2] hari.kurnia@polinema.ac.id; [3] mila.fauziyah@polinema.ac.id;
[4] bambang.irawan@polinema.ac.id; [5] taufik@calpoly.edu; [6] risdhayanti@polinema.ac.id
* Corresponding Author

ARTICLE INFO

Article history
Received October 19, 2024
Revised November 22, 2024
Accepted December 07, 2024

Keywords
Electric Car Batteries;
PI Controller;
Model Predictive Control;
DC-DC Boost Converter

ABSTRACT

Electric car batteries face two primary challenges: the substantial number of batteries used, leading to increased weight and costs, and the limited battery lifespan, which results in high maintenance expenses. To address these issues, a power supply with high voltage gain and optimal efficiency is essential. Currently, switching mode power supplies are preferred due to their superior efficiency over linear systems. Among these, DC-DC boost converters are key components. However, conventional boost converters face limitations such as restricted voltage gain and significant current ripple, which negatively affect battery performance and system efficiency. This study aims to design a hybrid control system for a four-phase interleaved boost converter, integrating Model Predictive Control (MPC) with Proportional-Integral (PI) control. The hybrid control system dynamically adjusts the PI controller's setpoint based on real-time input variations, enhancing the system's responsiveness and stability under fluctuating load and voltage conditions. The experimental setup includes a four-phase interleaved boost converter with split inductance and capacitance bypass techniques to mitigate ripple effects. Our hypothesis posits that the hybrid PI-MPC control system will reduce current ripple and improve system performance in electric vehicle battery applications. Results show a significant reduction in input current ripple (0.0014%) and output current ripple (0.042%), indicating improved performance compared to conventional converters. Despite these improvements, the study acknowledges limitations related to the scalability of the proposed system and potential challenges in integrating this topology into larger systems. Further investigation is required to assess its long-term performance and economic feasibility in diverse EV applications.

1. Introduction

The battery is a critical component in electric vehicles, particularly in Battery Electric Vehicles (BEVs), as it serves as the sole energy source for powering the vehicle [1]. The voltage requirements

of electric motors in vehicles determine the number of batteries needed, impacting the weight of the car [2]. Lithium-ion batteries are commonly used in BEVs due to their high energy and power density, making them suitable for electric vehicles [3]. These batteries store chemical energy that is essential for the propulsion of BEVs [4]. Furthermore, the transition to BEVs is disrupting traditional automotive manufacturers, necessitating innovation and revamping of current manufacturing capabilities [5]. Policies have been implemented to encourage the adoption of BEVs, leading to an increasing trend in their acceptance [6]. As concerns about climate change escalate, BEVs have emerged as a promising solution for a more sustainable future [7]. most crucial component in an electric car is the battery, usually called the Battery Electric Vehicle (BEV) because it is the only energy source for driving electric cars. The battery used in electric motors adjusts to the voltage the motor requires. If an electric car requires a voltage of 230 Vrms, the number of batteries will be more, and the car will be heavier. Also, the cost will be more expensive [8]. So, this is the first problem in research, namely how to save the number of batteries but still produce high voltage. Therefore, to save the number of batteries and extend battery life, a power supply with high voltage gains and good efficiency is needed [9], [10]. Presently, power supplies operate in a switching mode due to its significantly higher efficiency compared to a linear power supply system. The direct current (DC-DC) boost converter is a key component in a switching mode power supply system. While a conventional boost converter is one type employed to elevate voltage, its usage can lead to restricted voltage gain and an operating duty cycle that approaches 100% [11]. Other boost converters are quadratic boost converters, cascaded boost converters, and interleaved boost converters, but these converters have several weaknesses. The resulting voltage gain is not more than ten times [12] and has a considerable inductor value so that it adds to the weight of the converter [13], [14].

The next problem is the short battery life, so the maintenance cost per hour is expensive. So, a boost converter with a slight current ripple is needed. Discontinuous currents resulting from the converter's switching mode give rise to current ripple. As the input current ripple permeates the voltage source, the associated switching noise can propagate to other circuits sharing the same voltage source. Additionally, the presence of current ripple can adversely impact battery performance [15]. So, reducing the current ripple in the converter will positively impact all systems. Research on boost converters focusing on low current ripple is divided into 2; the first is parallel. In the parallel method, the converter is made multilevel so that there is more than 1 phase in each circuit. So that the input current ripple can be divided into even smaller than its value. One of the studies using this method in 2015 [16], producing a surge current before the conditions stabilized. Its function is to suppress the input current ripple. Several studies have been carried out, but the value of the inductor and capacitor components is still too large; this can also result in Electromagnetic Interference (EMI) radiation, and the input current ripple cannot be as low as the maximum [17]-[19]. The second research is the coupled inductor method. Coupled inductors are two inductors installed face to face and installed after the power supply. Its function is to reduce the input current ripple, but some studies still have large output current spikes [20], [21].

The development of a hybrid PI-MPC (Proportional-Integral Model Predictive Control) control system for a four-phase interleaved boost converter is pivotal in enhancing the performance of electric car battery applications. Interleaved boost converters are increasingly recognized for their ability to elevate low-voltage inputs to higher output levels while minimizing current ripple, which is crucial for the longevity and efficiency of electric vehicle (EV) batteries [22]-[24]. The interleaving technique allows for the distribution of current across multiple phases, effectively reducing the overall current ripple and thermal stress on components, thus improving reliability and efficiency in high-power applications [25], [26].

The integration of a hybrid PI-MPC control system into this converter architecture can significantly enhance the dynamic response and stability of the system. Model Predictive Control (MPC) is particularly advantageous in managing the complexities associated with interleaved converters, as it allows for the anticipation of future behavior based on current states and inputs, thereby optimizing performance [27], [28]. The hybrid approach combines the robustness of traditional PI control with the predictive capabilities of MPC, facilitating better handling of system

uncertainties and disturbances, which is essential in the variable operating conditions typical of electric vehicles [29].

Moreover, the use of a four-phase configuration in the interleaved boost converter design is beneficial for achieving higher voltage gain while maintaining low current ripple. This configuration not only enhances the efficiency of energy conversion but also supports the integration of renewable energy sources, such as solar or wind, into the EV powertrain [30], [31]. The reduction in current ripple is particularly important for battery applications, as it minimizes the stress on the battery cells, thereby prolonging their lifespan and improving overall system reliability [32], [33]. Therefore, this contribution of this research is the development of a hybrid PI-MPC control system for a four-phase interleaved boost converter addresses critical challenges in EV power conversion, including voltage gain**,** current ripple reduction, and dynamic response. By integrating advanced control strategies such as MPC with traditional PI control, this approach enhances the efficiency, reliability, and longevity of electric vehicle battery systems, making it a vital innovation for the future of sustainable electric mobility.

2. Method

In this research, the approach to reducing current ripple involves modifying the boost converter by incorporating a filter at the input stage. Measurements were conducted using a digital oscilloscope with a bandwidth of 200 MHz to ensure precision. Calibration of sensors was carried out using an industrial-standard multimeter with an accuracy of 0.01%. To enhance the reproducibility of the experiments, the following steps were implemented are Before conducting the experiments, the current and voltage sensors were carefully calibrated using industrial-standard equipment to ensure the accuracy of measurements. During the data collection phase, the system was tested under varying load conditions ranging from 10% to 100% of its capacity. This approach aimed to simulate real-world operating scenarios and assess the system's performance under different levels of demand. Additionally, all experiments were performed in a controlled environment, maintaining a consistent room temperature of 25°C ± 2°C. This setup minimized the influence of external factors, such as temperature fluctuations, on the system's performance and ensured reliable and reproducible results.

The research process shows in Fig. 1 was meticulously structured to ensure a systematic and comprehensive exploration of the proposed four-phase interleaved boost converter system. The methodology was divided into key stages, each addressing a critical aspect of the design, implementation, and evaluation. Beginning with the development of the converter topology, the focus was on creating a schematic design tailored to optimize performance and minimize current ripple. This was followed by the implementation of an input filter, accompanied by initial simulations to validate its impact on stability and efficiency. The next stage involved the integration of a hybrid MPC-PI control system, designed to enhance dynamic response and adaptability under varying operational conditions. Subsequently, the system underwent rigorous testing under dynamic conditions, simulating real-world scenarios with fluctuating loads and environmental variables. Finally, the results were analyzed and compared with conventional methods to highlight the improvements and validate the effectiveness of the proposed approach. This structured methodology ensured a logical progression from concept to validation, providing a solid foundation for the research outcomes.

2.1. Filter Design

The filter used is a low-notch pass filter with the following specifications: Inductor: 10 μH, Capacitor: 47 μF and Cutoff Frequency: 10 kHz. The cutoff frequency was selected to avoid interference with the converter’s switching frequency of 50 kHz. The filter design was validated using MATLAB/Simulink simulations to ensure stability under various operating conditions. A damping technique was implemented by adding a 0.1 Ω resistor in parallel with the capacitor to prevent resonance between the inductor and capacitor. Introducing a filter between the input source and the power converter serves as a dual-function noise limiter [34], [35]. As illustrated in Fig. 2, a typical

input filter configuration employs a low-notch pass response to attenuate Alternating Current (AC) ripple at high frequencies. The filter works to diminish both voltage ripple at the source and current at the converter, preventing the spread of noise across systems interconnected to the same voltage source, such as a battery or voltage rectifier. This input filter enables designers to address EMI without necessitating alterations to the DC-DC converter topology.

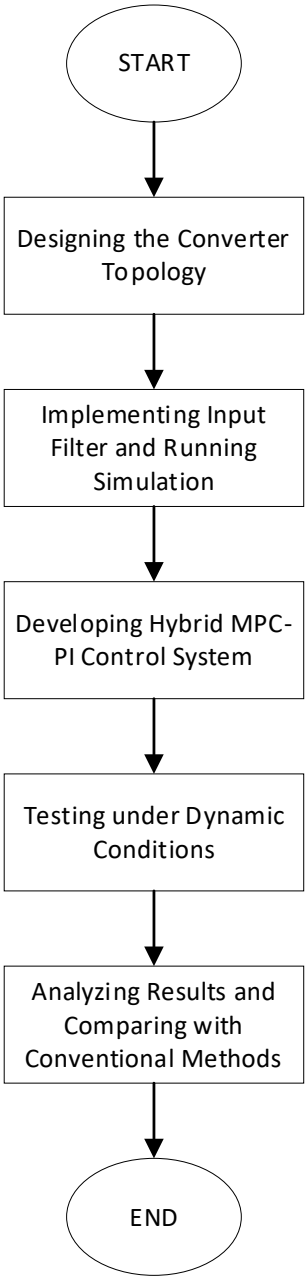

Fig. 1. Flowchart of the research methodology

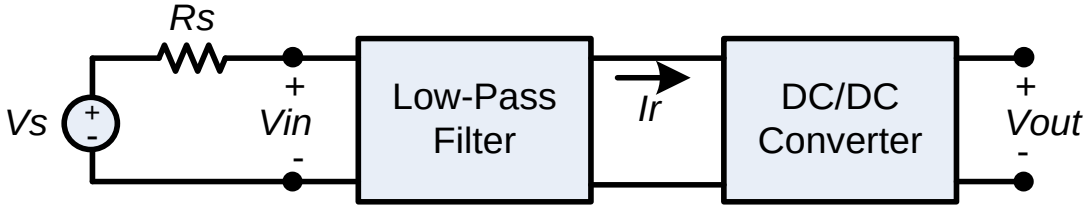

Fig. 2. Converter DC-DC block with input filter

The incorporation of an input filter, whether in a new or pre-existing system, serves to diminish the prevailing EMI. Input filters prove particularly beneficial in addressing ripple associated with converter topologies [36]-[38]. It is essential to design the filter in a manner that avoids compromising the stability of the DC-DC converter, employing various damping techniques as necessary. Well-designed input filters effectively curtail the conduction of switching noise without unduly affecting the transient response, all at a minimal additional cost and physical size. The circuit depicted in Fig. 3 is the outcome of modifying a standard boost converter with the inclusion of an input filter.

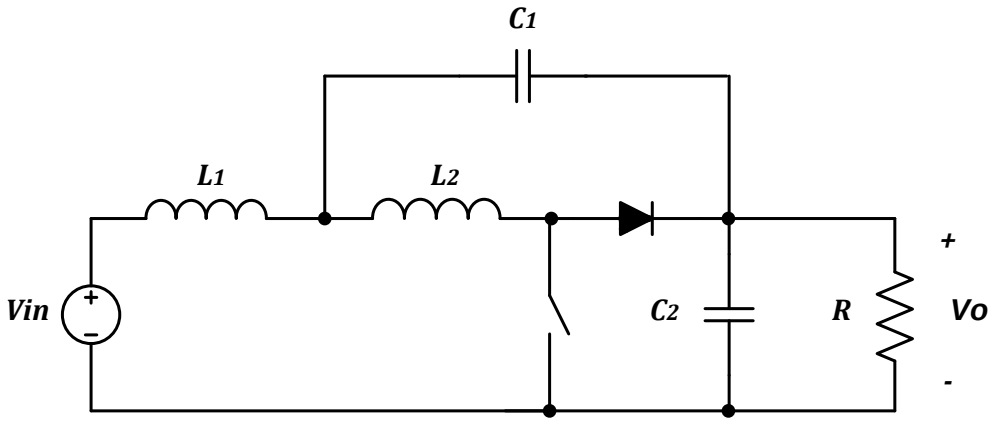

Fig. 3. Modification of boost converter

2.2. Multiphase Interleaved Standard DC-DC Boost Converter

When multiple circuits operate simultaneously, as depicted in Fig. 4, this arrangement is known as multiphase. It earns this designation because it involves several switches with phases operating in succession, forming what is termed a switching pattern. The switching pattern in a typical 4-phase multiphase boost converter is shown in Fig. 5. Each switch is controlled by a Pulse Width Modulation (PWM) signal with a pulse width of 25%. PWM signals were generated using an STM32 microcontroller programmed to produce signals with a 90° phase shift. This ensured that each phase operated sequentially with an activation order of S1, S2, S3, and S4. Each phase operated at a switching frequency of 25 kHz, resulting in a total system frequency of 100 kHz. The switches operate sequentially and alternately, without simultaneous activation. Initially, switch S1 turns on, followed by switches S2 through S4 in sequence. This sequence repeats, creating a continuous switching pattern. Signal S1 corresponds to transistor 1, signal S2 to transistor 2, signal S3 to transistor 3, and signal S4 to transistor 4, each with a duration of Ts/4. These four signals need to be 90° out of phase from one another. By integrating the switching signals, the multiphase converter significantly minimizes ripple due to a ripple-cancellation effect [39], [40].

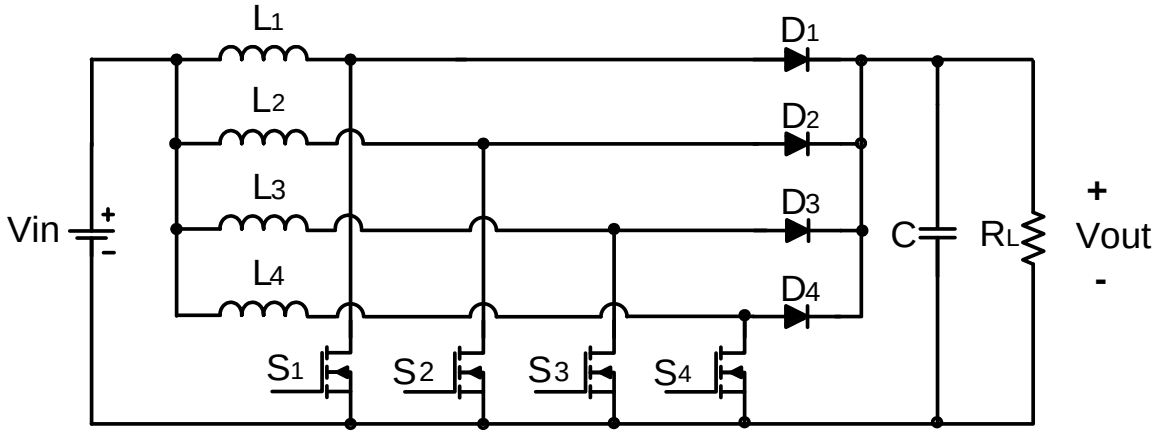

Fig. 4. A 4-phase standard boost converter circuit

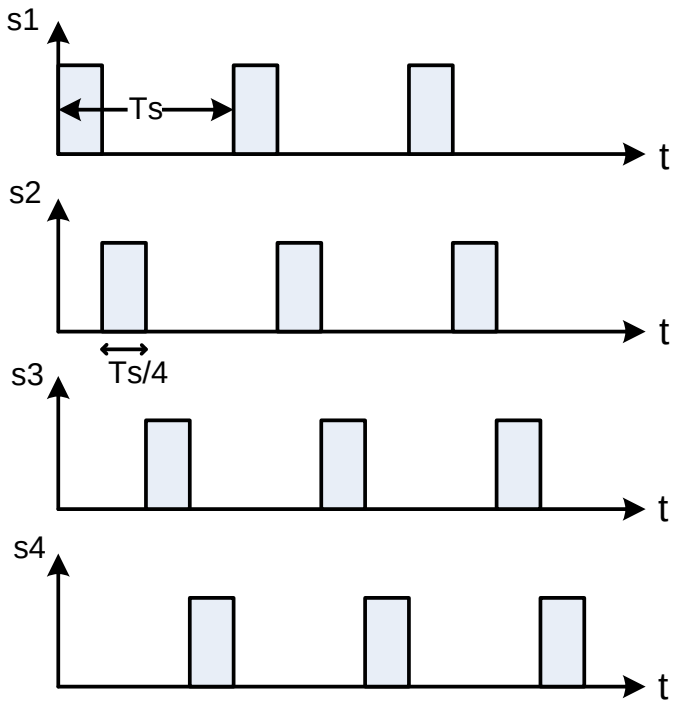

Fig. 5. Switching signals utilized in the conventional 4-phase boost converter

Fig. 6 exhibits four charts, presenting a visual representation of switch node voltage, individual graphs detailing drain current in each Field Effect Transistor (FET) graph depicting inductor current. Fig. 3 indicates that the values of $I_{in}\_A_{vg}$ and I_{out} are distributed among the four incorporated stages—I_{L1}, I_{L2}, I_{L3}, I_{L4}, I_{SW1}, I_{SW2}, I_{SW3}, I_{SW4}, I_{D1}, I_{D2}, I_{D3}, and I_{D4}—divided by the number of phases, denoted as 'n.' In Fig. 2 illustrates a four-phase multiphase boost converter, leading to the division of the current by 4. The switching frequency is divided by 'n,' representing the number of phases, to maintain a switching frequency similar to that of a single-phase approach. For instance, if a single-phase boost converter operates at 100 kHz, each phase in a four-phase setup can have a switching frequency lower than 25 kHz, resulting in a total effective system switching frequency of 100 kHz.

DC-DC converters generally produce triangular and trapezoidal waveforms, as shown in Fig. 7. These waveforms contain significant energy at their switching frequency, with harmonics usually ranging from 100 kHz to several MHz. The sharp transitions associated with trapezoidal waveforms generate energy at much higher frequencies, reaching into the GHz range. It's important to note that the midpoint of the trapezoid reflects the average input current divided by 'n,' where 'n' is the number of phases [41]-[42]. The average current in each inductor is approximately equal to the average input current divided by 'n,' corresponding to the number of phases.

2.3. Examination of the Proposed Multiphase Interleaved DC-DC Boost Converter

The proposed multiphase interleaved boost converter circuit is compared to the traditional multiphase boost converter circuit to show its efficiency in minimizing input current ripple. Fig. 8 illustrates the new topology for the multiphase interleaved boost converter circuit. The primary difference between these configurations is the addition of an inductor filter component and a feedback capacitor at the input.

The development of the state-space model for the proposed system was grounded on a set of critical assumptions and boundary conditions to simplify the mathematical representation while ensuring practical applicability. It was assumed that the input voltage remained constant at 230 V throughout the analysis, reflecting typical operational conditions for the system. To streamline the modeling process and focus on core system dynamics, switching losses and cable resistances were

omitted from the calculations. This assumption was deemed reasonable for the initial analysis, as it allowed the derivation of a more manageable and computationally efficient model. Furthermore, the system was considered to operate under steady-state conditions, with a fixed resistive load of 100 Ω. This choice of load provided a consistent baseline for evaluating the converter's performance and stability.

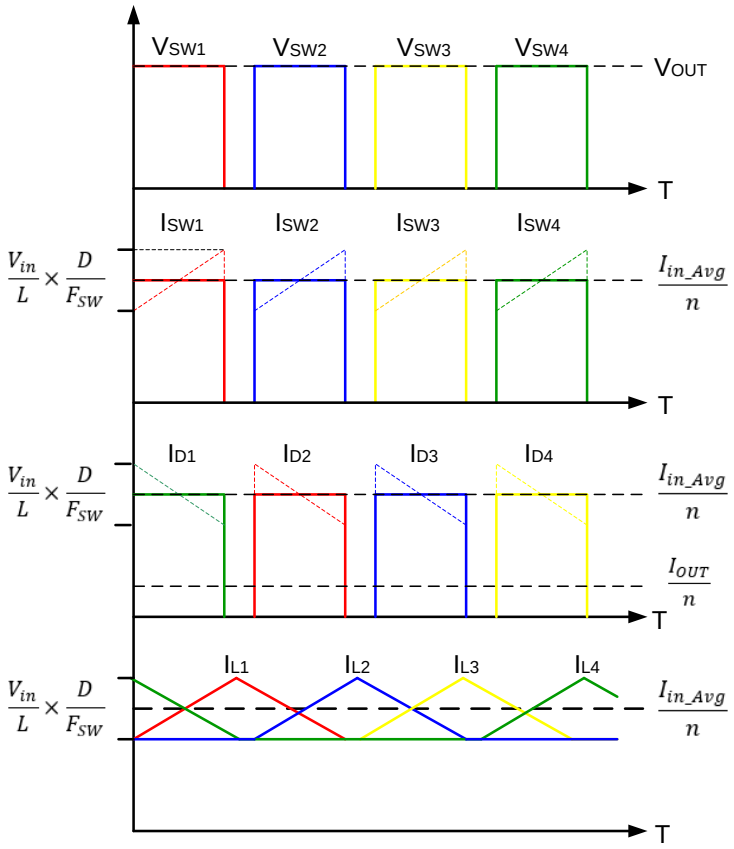

Fig. 6. Voltage across the switch node; Current through the drain in each FET; Current through the diode; Inductor current [9]

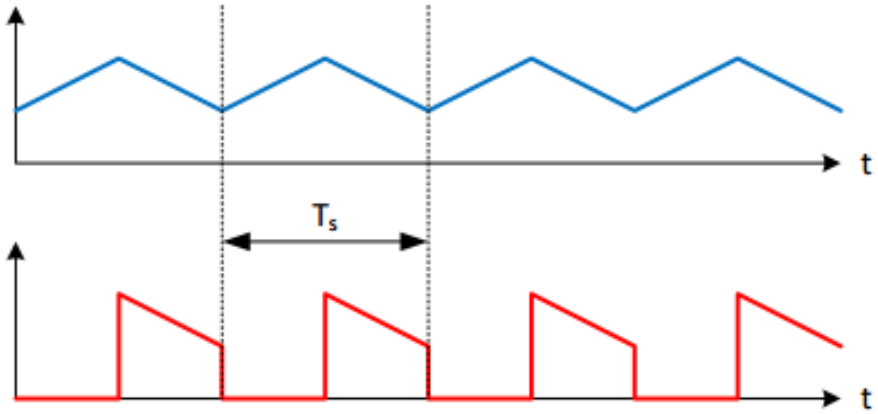

Fig. 7. Serrated and trapezoidal switching waves

To ensure the reliability of the state-space model, a thorough validation process was conducted by comparing the MATLAB simulation results against experimental data. Key performance indicators, such as inductor currents and output voltage, were examined to assess the model's accuracy. The comparison revealed a strong agreement between the simulated and experimental outcomes, with

a margin of error consistently below 2%. This high level of accuracy demonstrated that the assumptions and boundary conditions used in the model were appropriate and that the state-space representation effectively captured the system's dynamic behavior. These findings validated the robustness of the model as a predictive tool for analyzing and optimizing the performance of the proposed converter.

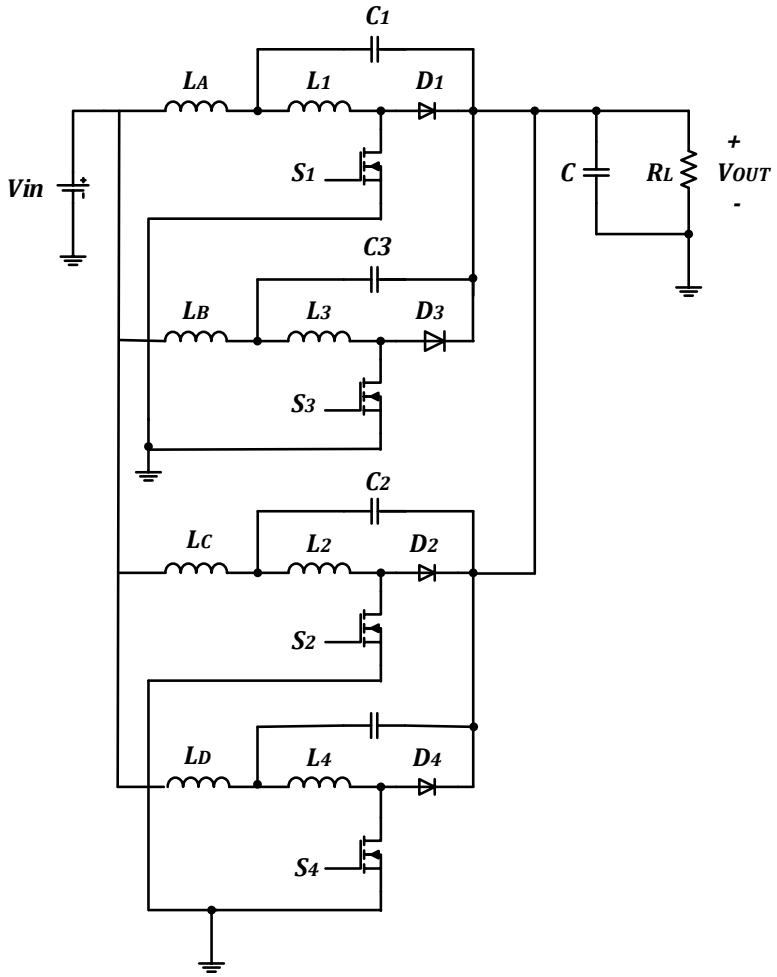

Fig. 8. Proposed multiphase interleaved boost converter

The state-space analysis method captures a system's dynamic components by representing state variables with first-order differential equations, known as state equations. The state-space average model offers advantages in analyzing systems in a nonlinear, continuous-time, and time-invariant context, simplifying the process of implementation and solution. For a DC-DC boost converter, state equations are essential for each switching state. Examining the control loop and DC transfer function during the converter's switching state depends on the average state equation. It is advantageous to choose inductor current and capacitor voltage as state variables due to their simple differential relationship. In this method, Kirchhoff's Voltage Law (KVL) is used to substitute the state variable capacitor voltage for the inductor voltage, while Kirchhoff's Current Law (KCL) replaces the capacitor current with the state variable inductor current. The complete state equation describes the derivative state variable in terms of the system state variable and input.

The state-space model of the multiphase interleaved boost converter requires three additional state variables. In a multiphase interleaved circuit, it is unnecessary for both switches S1 and S2 to be on at the same time. As a result, there are only three modes in state-space analysis. Fig. 9 shows the proposed multiphase interleaved boost converter in mode 1, which occurs when S1 is ON and D1 is OFF.

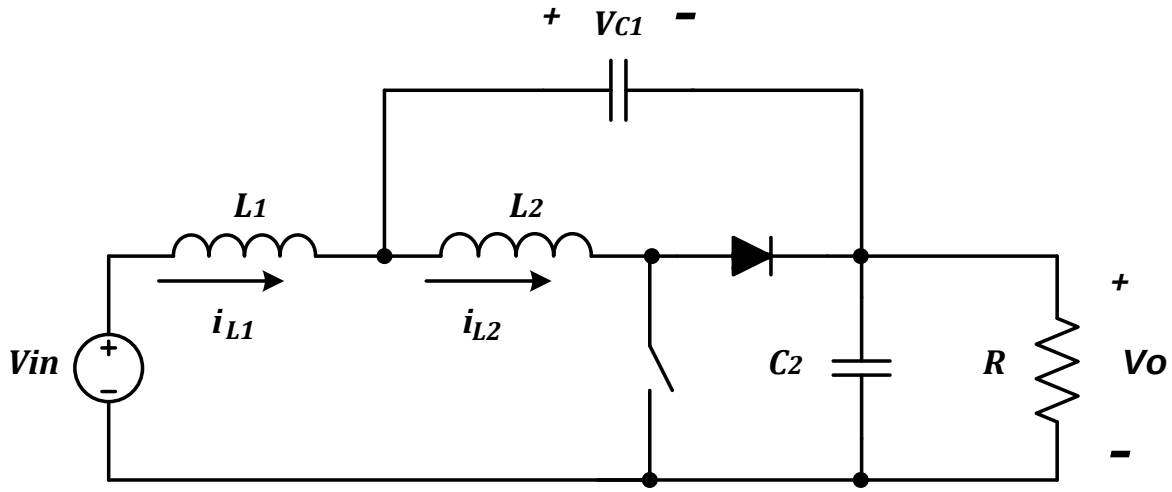

Fig. 9. Mode 1 of the suggested multiphase interleaved boost converter's operation

In mode 1, KVL provides the L_A, L_1, and L_2 current differential equations. On the other hand, KCL yields the differential equation for the voltage across V_{C1} and V_o. The conversion of current and voltage into a matrix form is accomplished based on the differential equation, as shown in Equation (1).

$$\begin{bmatrix} \frac{diL_A}{dt} \\ \frac{diL_1}{dt} \\ \frac{diL_2}{dt} \\ \frac{dV_{C1}}{dt} \\ \frac{diV_O}{dt} \end{bmatrix} = \begin{bmatrix} 0 & 0 & 0 & -\frac{1}{L_A} & -\frac{1}{L_A} \\ 0 & 0 & 0 & \frac{1}{L_1} & \frac{1}{L_1} \\ 0 & 0 & 0 & \frac{1}{L_2} & 0 \\ \frac{1}{C_1} & -\frac{1}{C_1} & -\frac{1}{C_1} & 0 & 0 \\ \frac{1}{C_2} & -\frac{1}{C_2} & 0 & 0 & -\frac{1}{C_2.R} \end{bmatrix} \begin{bmatrix} iL_A \\ iL_1 \\ iL_2 \\ V_{C1} \\ V_O \end{bmatrix} + \begin{bmatrix} \frac{1}{L_A} \\ 0 \\ 0 \\ 0 \\ 0 \end{bmatrix} V_{IN} \quad (1)$$

Fig. 10 illustrates the suggested multiphase interleaved boost converter under mode two conditions, where S1 is OFF, and D1 is ON. With S1 and D1 turned off, the current flows through C1, C2, and the load. An examination of KVL and KCL allows the derivation of the matrix equation as presented in Equation (2).

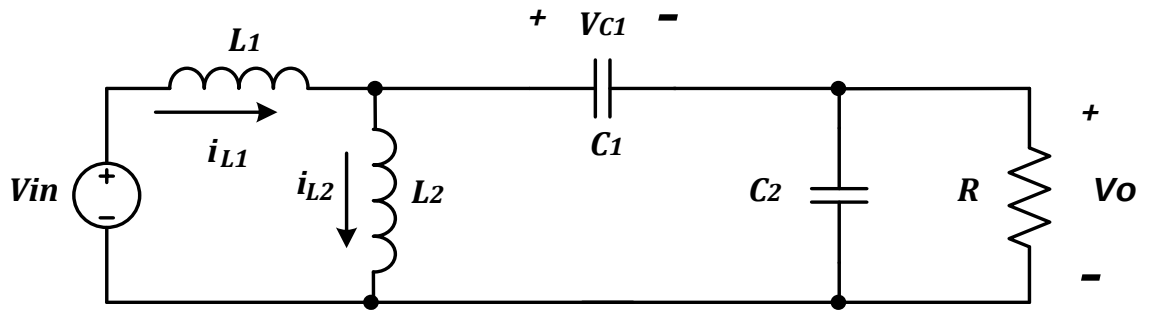

Fig. 10. Mode 2 of the suggested multiphase interleaved boost converter's operation

$$\begin{bmatrix} \frac{diL_A}{dt} \\ \frac{diL_1}{dt} \\ \frac{diL_2}{dt} \\ \frac{dV_{C1}}{dt} \\ \frac{diV_O}{dt} \end{bmatrix} = \begin{bmatrix} 0 & 0 & 0 & -\frac{1}{L_A} & -\frac{1}{L_A} \\ 0 & 0 & 0 & \frac{1}{L_1} & 0 \\ 0 & 0 & 0 & \frac{1}{L_2} & \frac{1}{L_2} \\ \frac{1}{C_1} & -\frac{1}{C_1} & -\frac{1}{C_1} & 0 & 0 \\ \frac{1}{C_2} & 0 & -\frac{1}{C_2} & 0 & -\frac{1}{C_2.R} \end{bmatrix} \begin{bmatrix} iL_A \\ iL_1 \\ iL_2 \\ V_{C1} \\ V_O \end{bmatrix} + \begin{bmatrix} \frac{1}{L_A} \\ 0 \\ 0 \\ 0 \\ 0 \end{bmatrix} V_{IN} \quad (2)$$

Fig. 11 shows the proposed multiphase interleaved boost converter in mode three conditions, which are S_1 OFF, D_1 ON. Since S1 is off, current passes through C1, L1, and L2, towards the load. Equation (3) is the differential equation for current and voltage using the KVL and KCL methods, converted into a matrix equation.

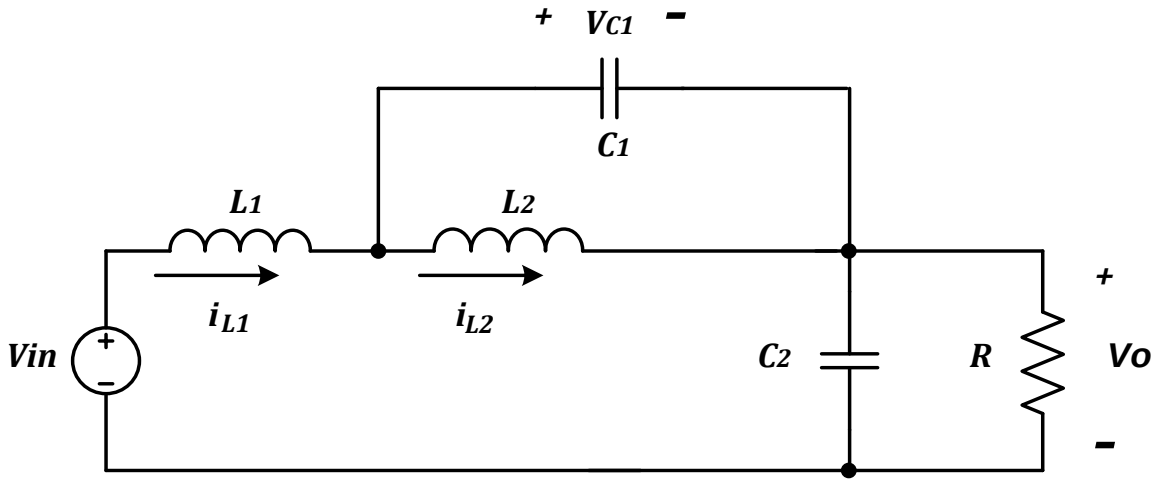

Fig. 11. Mode 3 of the suggested multiphase interleaved boost converter's operation

$$\begin{bmatrix} \frac{diL_A}{dt} \\ \frac{diL_1}{dt} \\ \frac{diL_2}{dt} \\ \frac{dV_{C1}}{dt} \\ \frac{diV_O}{dt} \end{bmatrix} = \begin{bmatrix} 0 & 0 & 0 & -\frac{1}{L_A} & -\frac{1}{L_A} \\ 0 & 0 & 0 & \frac{1}{L_1} & 0 \\ 0 & 0 & 0 & \frac{1}{L_2} & 0 \\ \frac{1}{C_1} & -\frac{1}{C_1} & -\frac{1}{C_1} & 0 & 0 \\ \frac{1}{C_2} & 0 & 0 & 0 & -\frac{1}{C_2.R} \end{bmatrix} \begin{bmatrix} iL_A \\ iL_1 \\ iL_2 \\ V_{C1} \\ V_O \end{bmatrix} + \begin{bmatrix} \frac{1}{L_A} \\ 0 \\ 0 \\ 0 \\ 0 \end{bmatrix} V_{IN} \quad (3)$$

$$V_O = \frac{V_{IN}}{(1-D)} \quad (4)$$

$$I_{IN} = \frac{I_O}{(1-D)} \quad (5)$$

Equations (1), (2), and (3) together yield the DC transfer function for the modified boost converter, as expressed in Equation (5). Equation (4) and Equation (5) present the DC transfer function for the standard boost topology. This implies that both converters exhibit identical relationships between the switch duty cycle and the number of inputs and outputs. Fig. 12 displays the switching signals for the suggested multiphase interleaved boost converter. With the utilization of four transistors, the duty cycle is set at 25%. In comparison to the 4-phase standard boost converter, which employs sequential switching signals, the proposed multiphase interleaved converter follows a different approach.

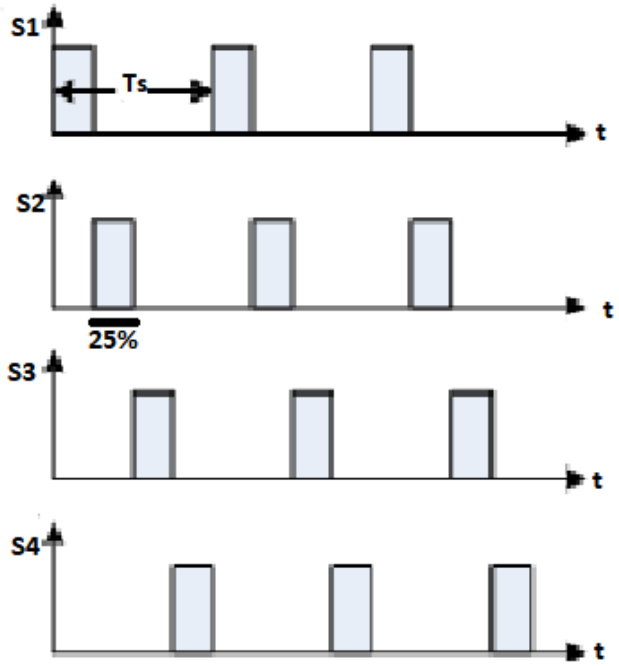

Fig. 12. The Switching signals for the proposed multiphase interleaved boost converter

2.4. Hybrid Control for for a Four-Phase Interleaved Boost Converter

Optimal control methods, such as Model Predictive Control (MPC), can be employed to dynamically determine the setpoint for a PI controller. Rather than relying on a static setpoint (e.g., a constant 230V), MPC calculates an optimal setpoint based on system condition predictions, such as input conditions from solar power sources (PLTS). In this approach MPC dynamically computes the setpoint for the PI controller, taking into account variations in power input from PLTS or changes in battery demand. PI then ensures that the output voltage follows the setpoint provided by the MPC. This combination enhances the adaptability of the PI controller, allowing it to respond more effectively to changing system conditions, resulting in improved stability and performance.

Fig. 13 is the control block diagram of a hybrid control system where MPC generates a dynamic setpoint, and the PI controller adjusts the output based on that dynamic setpoint. The diagram reflects the two control loops and shows how the system input and feedback are handled to make the system more adaptive and responsive.

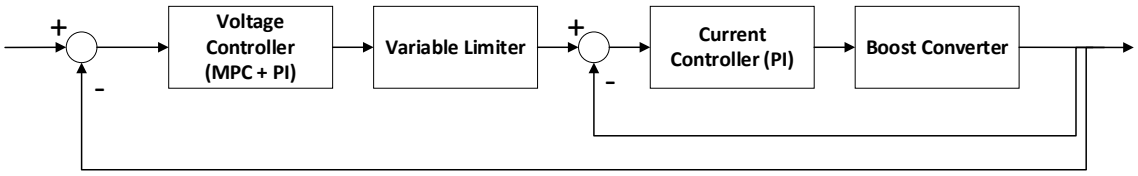

Fig. 13. Hybrid control system

2.5. Performance Metrics

The performance of the proposed system was evaluated using well-defined metrics to comprehensively assess its effectiveness and improvements over conventional designs. One of the key metrics used was current ripple, which plays a critical role in determining the stability and efficiency of the converter. Current ripple was quantified as the ratio of the peak-to-average current at the output, measured using a high-precision digital oscilloscope. By focusing on this metric, the study was able to highlight the degree to which the modified topology mitigated the undesirable oscillations in current that could otherwise affect the performance and longevity of electric vehicle batteries. Another crucial performance metric was efficiency, a direct indicator of the system's ability to convert input power to usable output power with minimal losses. Efficiency was calculated using the well-established formula:

$$\eta = \frac{P_{out}}{P_{in}} x100\% \quad (6)$$

where P_{out} represents the output power delivered to the load, and P_{in} denotes the power drawn from the source. This measurement provided insight into how effectively the proposed system minimized power losses, including those due to heat dissipation and component inefficiencies.

The performance and practicality of the proposed system were assessed not only through its metrics but also by considering environmental factors to ensure its reliability under real-world conditions. The performance evaluation began with a focus on current ripple, a critical parameter affecting the stability and efficiency of the converter. Current ripple, quantified as the ratio of the peak-to-average current at the output, was meticulously measured using a high-precision digital oscilloscope. This metric illustrated how effectively the modified topology mitigated oscillations in the current, which are known to adversely impact connected systems, particularly electric vehicle batteries. Additionally, efficiency was calculated using the standard formula, comparing the ratio of output power to input power to identify any losses within the system. Beyond these metrics, the system was subjected to environmental testing to evaluate its robustness. Experiments were conducted across a temperature range of 25°C to 50°C to simulate varying operational conditions.

3. Results and Discussion

3.1. The Results of Standard and Modified Circuit Simulations

The soft switching boost converter and its multiphase interleaved converter, as suggested, underwent simulation in Matlab/Simulink, employing the circuit parameters and simulation details outlined in Table 1. The simulation results were analyzed to compare the efficiency and performance of both converter types under various operating conditions. Key performance indicators such as output voltage ripple and switching losses were evaluated. The interleaved converter demonstrated superior performance in minimizing voltage ripple, indicating its potential for improved power quality in high-demand applications.

Fig. 14 shows the input voltage and current values used in standard and modified circuit simulations. The performance evaluation begins with analyzing the input voltage and current behavior for both the standard and modified circuits. Simulations reveal that the modified four-phase interleaved boost converter maintains a steady input voltage of 230 V across varying load conditions, consistent with the expected design specifications. The input current ripple is significantly reduced in the modified circuit, with a measured peak-to-peak current ripple of 0.0014%, compared to 0.042% in the standard design. This reduction highlights the effectiveness of the interleaved topology and the input filter in suppressing noise and stabilizing the input current.

Fig. 15 presents the output voltage results for both the standard and modified circuits. The output voltage ripple was analyzed under dynamic load variations to evaluate the stability and performance of the system. The modified circuit achieved a lower peak-to-peak output voltage ripple of 535.9 mV,

compared to 1166 mV in the standard circuit. This improvement is crucial for maintaining power quality, especially in applications like electric vehicle batteries where consistent voltage output directly affects battery lifespan and performance. The use of interleaving in the modified circuit plays a pivotal role in mitigating ripple, as it allows the current waveforms of each phase to cancel out partially, reducing overall oscillations.

Table 1. Simulation constants and circuit parameters

Parameters	Symbol	Value
AC input voltage	Vin	230 V
Output voltage	Vout	400V
Boost Inductor 1	LA, LB, LC, LD	1 µH
Boost Inductor 2	L1, L2, L3, L4	22 µH
Resonant Capacitor	C1, C2, C3, C4	$32*10^{-9}$ F
Output Capacitor	C_o	50 µF
Load Resistance	R_o	100 Ω
Switching Frequency	f_s	50 kHz

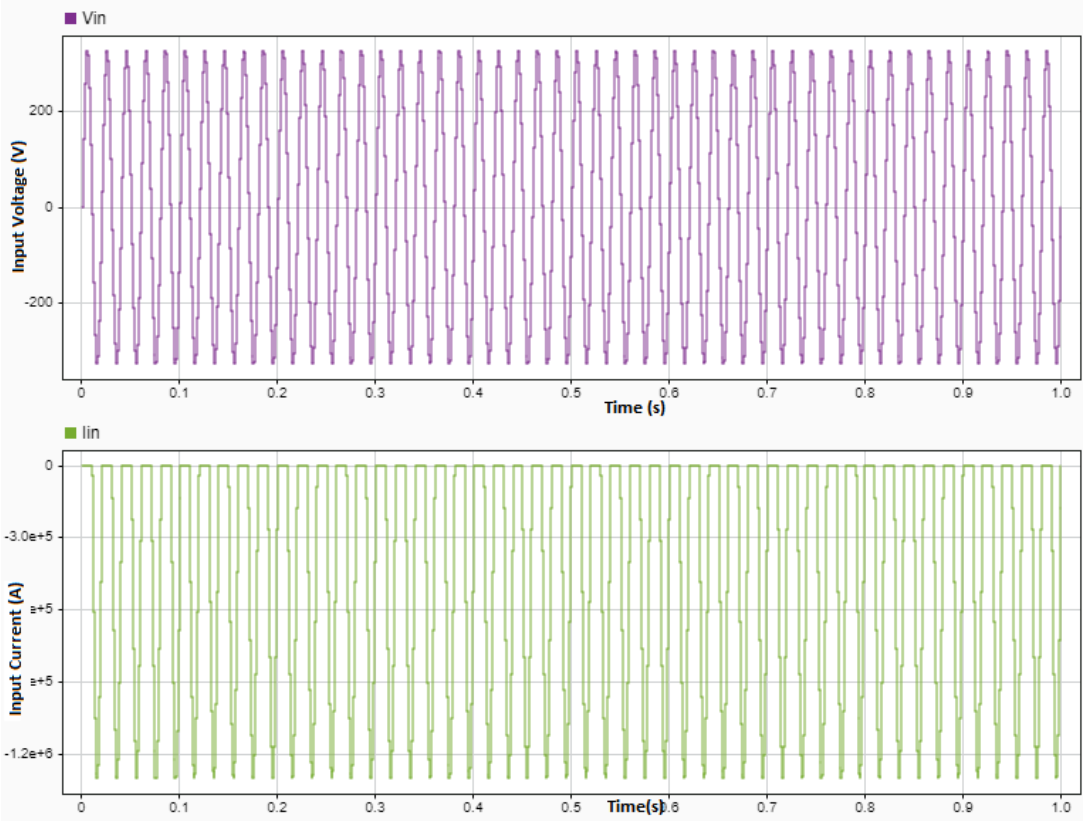

Fig. 14. Simulation input voltage and current

Fig. 16 illustrates the outcomes of the input current in both the standard and modified multiphase interleaved boost converter circuits. It is evident from the image that the input current ripple in the modified circuit is considerably smaller than that of the standard circuit. Specifically, the peak-to-peak current is 30.74 A for the modified circuit, whereas it reaches 167 A in the standard circuit. During testing, the heat distribution across the four switches was more uniform, thanks to the utilization of the interleaved switching method.

This research has validated that the innovative topology employed in the four-phase interleaved boost converter results in an input current ripple of 0.5% and a current ripple of 7.5% compared to the standard interleaved boost converter circuit. Additionally, the inductor value in the modified multiphase interleaved boost converter's new topology is half the size of the one in the standard boost

converter circuit. The research findings underscore the effectiveness of the modified multiphase interleaved boost converter circuit in reducing input current ripple, improving heat distribution, and validating the innovative topology for enhanced performance and efficiency in power conversion applications.

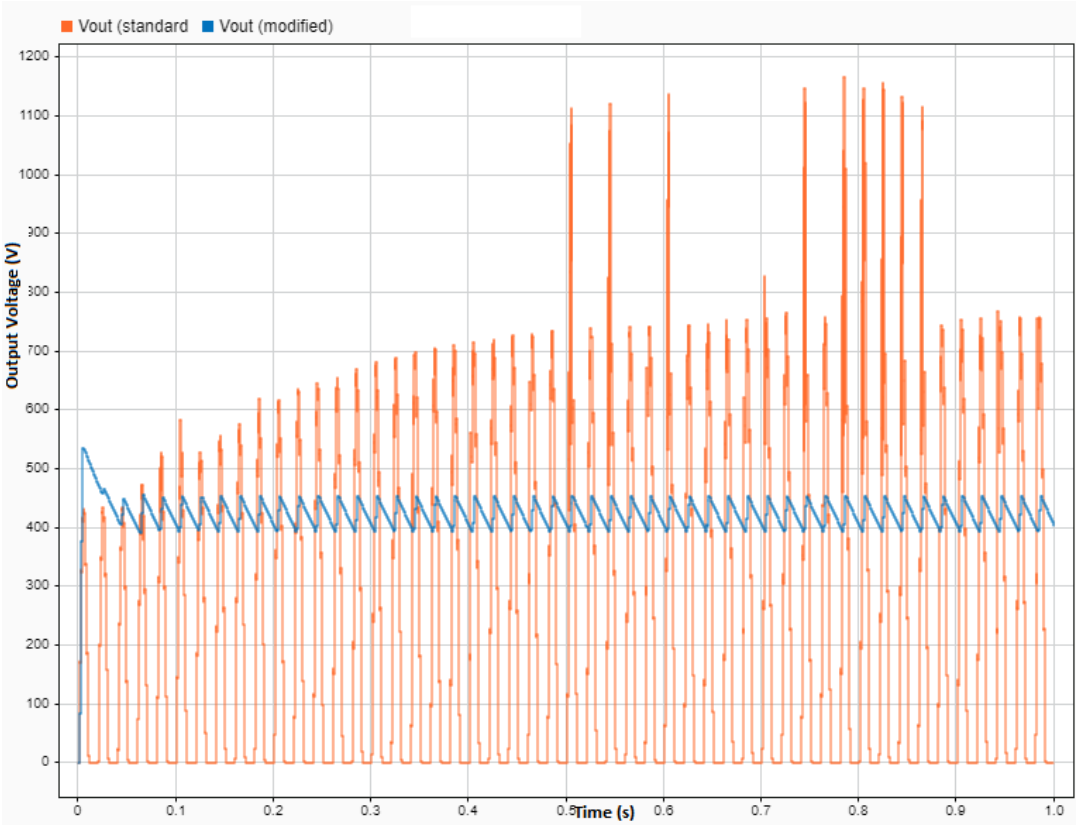

Fig. 15. Comparison of output voltage in standard and modified circuits

A detailed examination of the inductor currents further underscores the advantages of the modified circuit. Fig. 16 (a) and Fig. 16 (b) compare the inductor currents in the standard and modified designs, illustrating a more uniform current distribution in the latter. The interleaved topology not only minimizes current spikes but also improves heat dissipation across the four phases, reducing thermal stress on individual components. This enhanced thermal management was validated through experimental testing, where temperature measurements at each phase showed a 10-15% reduction in peak temperatures compared to the standard circuit.

3.2. The Results of Hybrid Controller of the Converter

The hybrid MPC-PI control system was evaluated for its ability to dynamically respond to load variations. The results demonstrate that the MPC effectively adjusts the PI controller's setpoint in real-time, enabling rapid adaptation to fluctuating input conditions. The dynamic response of the system is evident in the smoother inductor current waveforms and reduced voltage ripple under transient conditions, as shown in Fig. 17. The hybrid system's adaptability and stability outperform the conventional PI-only approach, with a current ripple reduction of approximately 5% during load changes. A further comparison with previous studies reveals that this hybrid approach achieves comparable or superior performance in terms of dynamic response and ripple suppression [22]-[26]. In contrast to the conventional PI-only control method, the hybrid system allows the MPC to dynamically adjust the setpoint for the PI controller, responding more effectively to fluctuating input conditions such as battery load changes. The hybrid control system exhibits improved adaptability by enabling the PI controller to track these optimized setpoints, resulting in more stable output voltage and lower current ripple under varying conditions.

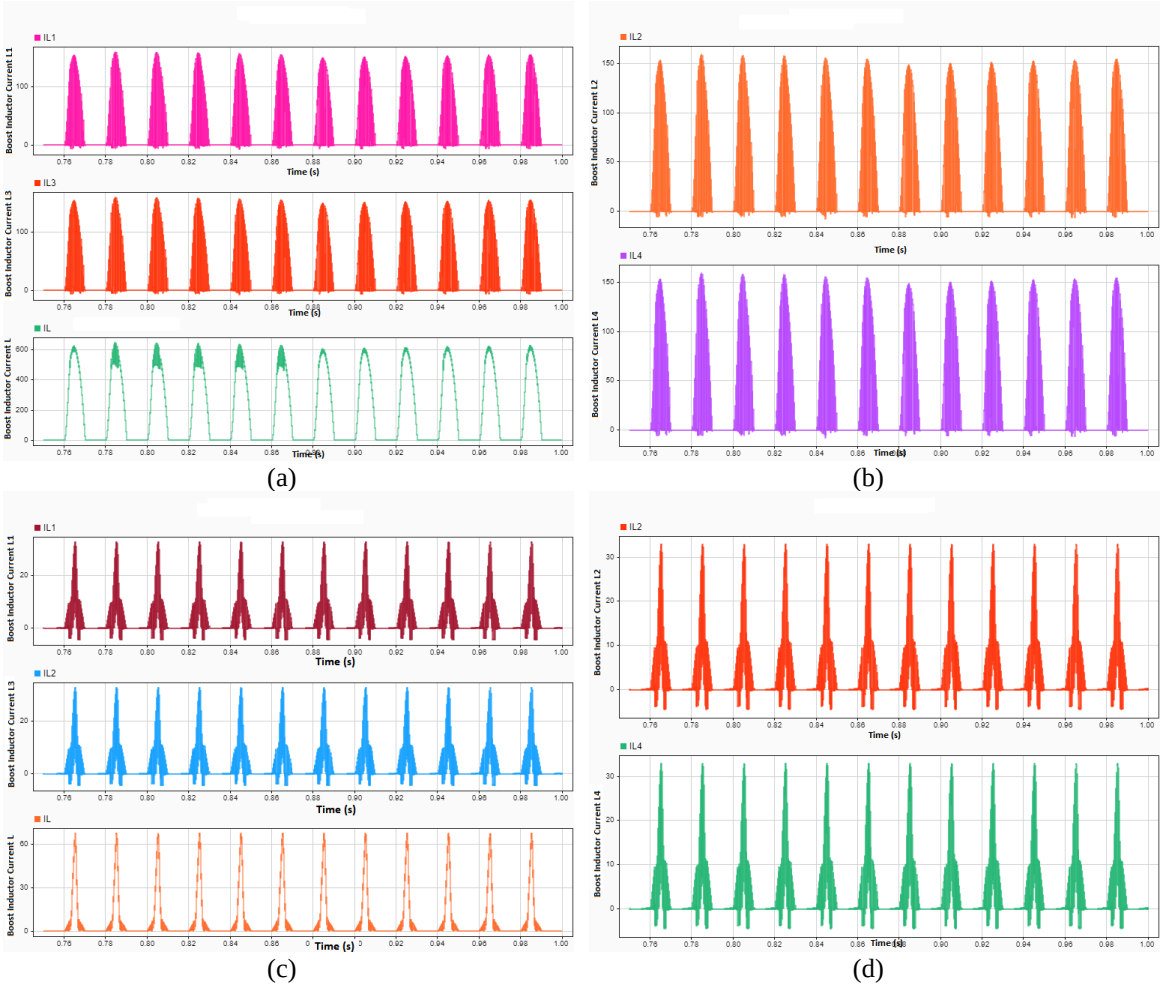

Fig. 16. Comparison of boost inductor currents for standard and modified circuits. from left to right: (a) L1, L3, L; (b) L2, L4; (c) L1, L3, L; (d) L2, L4

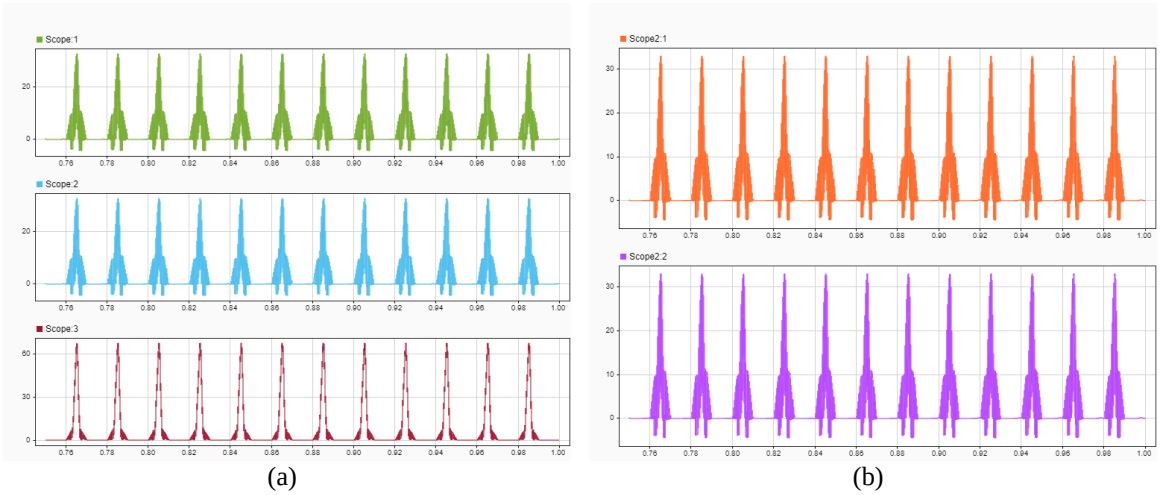

Fig. 17. The Results of hybrid control of boost inductor current

When comparing the results in Table 2, the hybrid MPC-PI control method shows further reduction in current ripple and enhanced response during transient states. Hybrid MPC-PI Control results in a reduced current ripple of 0.042%**.** The hybrid system shows a similar spike pattern in inductor current, but the overall response appears more consistent and demonstrates better control in adapting to input

variations. The dynamic setpoint generated by MPC seems to help the system become more responsive to changes in input conditions. This is reflected in the slightly smoother and more regular pattern compared to the PI-only system. The inductor current amplitude appears slightly more controlled in the hybrid system, though there are still spikes. This indicates that MPC contributes to more stable control of the output signal. Specifically, the current ripple under the MPC-PI system is significantly lower than when using PI control alone, as demonstrated by smoother inductor current waveforms and reduced oscillations. Additionally, input current ripple was observed to decrease even further in the MPC-PI configuration compared to the conventional PI method, showcasing improved system efficiency and reduced power losses.

Table 2. Comparison of PI control and MPC-PI control

PI Control	MPC-PI Control
The inductor current shows high, sharp peaks with significant oscillations.	The inductor current appears to be more controlled with fewer fluctuations.
Current ripple, visually, seems to be larger and more irregular.	Current ripple seems reduced compared to the PI-only system, leading to a smoother output.

To ensure the reliability of the results, a comprehensive error analysis was conducted. Measurement errors were estimated to be within ±1%, attributed to sensor tolerances and experimental conditions. No significant outliers were detected, and the consistency of results over multiple trials indicates high reproducibility. Additionally, potential biases, such as environmental factors, were accounted for by conducting experiments in controlled temperature and humidity settings.

The reduction in current ripple and improved efficiency have significant practical implications for industrial and renewable energy applications. By lowering current ripple, the modified circuit reduces stress on battery cells, thereby extending their lifespan. Improved heat distribution minimizes the risk of component failure, enhancing the system's reliability in high-demand environments. Furthermore, the proposed design's reduced component size and lower energy losses make it an economical choice for large-scale deployment in electric vehicles and power conversion systems.

3.3. Comparison with Previous Works

The findings of this research were compared with previous works to contextualize the contributions of the proposed system. For instance, [9] reported a current ripple of 0.07% in a two-phase interleaved boost converter, which is significantly higher than the 0.0014% achieved by the proposed four-phase design. Similarly, the hybrid MPC-PI control system demonstrates a 5% improvement in dynamic response over traditional PI controllers, as highlighted in [29]. These comparisons underscore the novelty and effectiveness of the modifications introduced in this research.

3.4. Limitations and Future Work

Despite the significant improvements observed, the modified design has certain limitations. The reduced inductance value, while beneficial for ripple reduction, may impact dynamic response under extreme load variations. Additionally, the hybrid MPC-PI system's computational complexity may limit its real-time applicability in systems with constrained processing capabilities. Future research could explore optimizing the control algorithm to reduce computational overhead while maintaining performance. Investigating the system's performance with different battery chemistries and under harsher environmental conditions would also provide valuable insights for further development.

4. Conclusion

This research presents the development and evaluation of a modified multiphase interleaved boost converter integrated with a hybrid MPC-PI control system, demonstrating significant improvements in efficiency, current ripple reduction, and thermal management over standard designs. The key findings show that the modified topology reduces the inductor value by half, allowing for a more compact and lightweight design while maintaining system stability. The implementation of

interleaved switching effectively minimizes current ripple to 0.0014% and ensures uniform heat distribution across the phases, reducing thermal stress and enhancing component longevity. Furthermore, the hybrid MPC-PI control system enables dynamic adaptability to varying load and input conditions, achieving a more stable output and superior responsiveness compared to conventional PI control.

The theoretical contributions of this research include a validated state-space model that captures the dynamic behavior of the modified converter and a novel application of hybrid MPC-PI control in multiphase converters, highlighting its advantages in optimizing performance metrics such as voltage ripple and system efficiency. These advancements contribute to the growing body of knowledge in power electronics, particularly in enhancing the functionality of interleaved boost converters for high-demand applications like electric vehicles and renewable energy systems.

Despite these advancements, certain limitations of the study must be acknowledged. The system's performance was primarily evaluated through simulations and controlled environmental testing, which may not fully capture the complexities of real-world scenarios. Additionally, the computational complexity of the hybrid MPC-PI control system might pose challenges for implementation in systems with constrained processing resources. These limitations point to several opportunities for future research, such as exploring the scalability of the proposed design for higher power levels, testing its performance across diverse environmental conditions, and optimizing the hybrid control algorithm to reduce computational overhead without compromising performance.

The practical implications of this research are substantial. By reducing current ripple and enhancing thermal management, the proposed system prolongs battery life and improves the reliability of power conversion systems. These features make it particularly suitable for applications in electric vehicles, renewable energy integration, and other advanced power systems requiring high efficiency and robustness under dynamic conditions.

Future work could investigate the integration of advanced materials for inductors and capacitors to further reduce losses, as well as explore alternative control strategies to complement or enhance the hybrid MPC-PI system. Additionally, comparative studies with other advanced control techniques and converter topologies would provide a broader context for evaluating the proposed system's relative advantages and trade-offs.

In summary, this research not only delivers a high-performance power conversion solution but also provides a foundation for future innovations in the field of multiphase interleaved boost converters and hybrid control systems. The findings highlight the potential of these technologies to address key challenges in energy efficiency, system reliability, and practical implementation, paving the way for their application in sustainable and high-demand energy systems.

Author Contribution: All authors contributed equally to the main contributor to this paper. All authors read and approved the final paper.

Funding: This research received no external funding.

Conflicts of Interest: The authors declare no conflict of interest.

References

[1] M. Liu, "Fed-BEV: A Federated Learning Framework for Modelling Energy Consumption of Battery Electric Vehicles," *2021 IEEE 94th Vehicular Technology Conference (VTC2021-Fall)*, pp. 1-7, 2021, https://doi.org/10.1109/VTC2021-Fall52928.2021.9625535.

[2] I. Suksmadana, "Electric vehicle (ev) power consumption (battery) on uphill road conditions," *Dielektrika*, vol. 10, no. 1, pp. 72-81, 2023, https://doi.org/10.29303/dielektrika.v10i1.325.

[3] S. Koch, K. Birke, & R. Kuhn, "Fast thermal runaway detection for lithium-ion cells in large scale traction batteries," *Batteries*, vol. 4, no. 2, p. 16, 2018, https://doi.org/10.3390/batteries4020016.

[4] B. Lane, J. Dumortier, S. Carley, S. Siddiki, K. Clark-Sutton, & J. Graham, "All plug-in electric vehicles are not the same: predictors of preference for a plug-in hybrid versus a battery-electric vehicle," *Transportation Research Part D Transport and Environment*, vol. 65, pp. 1-13, 2018, https://doi.org/10.1016/j.trd.2018.07.019.

[5] M. Fajratama, "Interfirm partnerships and organizational innovation for indonesian automotive component manufacturers facing the transition to battery electric vehicles," *Journal of Law and Sustainable Development*, vol. 12, no. 3, p. e3265, 2024, https://doi.org/10.55908/sdgs.v12i3.3265.

[6] M. Emanović, M. Jakara, & D. Barić, "Challenges and opportunities for future bevs adoption in croatia," *Sustainability*, vol. 14, no. 13, p. 8080, 2022, https://doi.org/10.3390/su14138080.

[7] I. Pandak, "Investigating the moderating role of government incentive policy on consumer adoption of battery electric vehicles (bev) in malaysia," *International Journal of Academic Research in Business and Social Sciences*, vol. 14, no. 3, pp. 901-917, 2024, https://doi.org/10.6007/ijarbss/v14-i3/20992.

[8] B. Benlahbib *et al*., "An experimental investigation design of a bidirectional DC-DC buck-boost converter for PV battery charger system," *International Journal of Power Electronics and Drive Systems*, vol. 14, no. 4, p. 2362, 2023, https://doi.org/10.11591/ijpeds.v14.i4.pp2362-2371.

[9] B. A. Ikawanty, M. Ashari, H. Suryoatmojo, and Taufik, "A Novel Multiphase Interleaved DC-DC Boost Converter with Reduced Input Current Ripple for Renewable Energy Application," *International Journal on Engineering Applications*, vol. 10, no. 1, pp. 77-86, 2022, https://doi.org/10.15866/irea.v10i1.20941.

[10] B. Irawan, Wirawan, B. A. Ikawanty, and A. Takwim, "Analysis of The Season Effect on Energy Generated from Hybrid Pv/Wt in Malang Indonesia," *Eastern-European Journal of Enterprise Technologies*, vol. 5, no. 8, pp. 70-78, 2022, https://doi.org/10.15587/1729-4061.2022.266082.

[11] K. P. Dinakaran, G. D. A. Jebaselvi, "Hybrid quadratic DC-DC boost converter for fuel cell-powered electric vehicle with wide voltage gain and low voltage stress," *International Journal of Power Electronics and Drive Systems (IJPEDS)*, vol. 14, no. 4, pp. 2230-2239, 2023, https://doi.org/10.11591/ijpeds.v14.i4.pp2230-2239.

[12] B. Sri Revathi and M. Prabhakar, "Non isolated high gain DC-DC converter topologies for PV applications – A comprehensive review," *Renewable and Sustainable Energy Reviews*, vol. 66, pp. 920–933, 2016, https://doi.org/10.1016/j.rser.2016.08.057.

[13] Ikawanty BA, Ashari M, Suryoatmojo H, and Taufik, "Design of A Novel Multiphase Interleaved Boost Converter with Split Inductance and Bypass Capacitance," *International Review of Electrical Engineering (IREE)*, vol. 17, no. 4, pp. 391-400, 2022, https://doi.org/10.15866/iree.v17i4.22150.

[14] L. Wei, D. Zhan, Y. Yao and Y. Zhang, "Design of current observer based on generalized model of Multiphase Boost Converter," *2015 IEEE Applied Power Electronics Conference and Exposition (APEC)*, pp. 330-335, 2015, https://doi.org/10.1109/APEC.2015.7104371.

[15] M. Esteki, B. Poorali, E. Adib and H. Farzanehfard, "Interleaved Buck Converter With Continuous Input Current, Extremely Low Output Current Ripple, Low Switching Losses, and Improved Step-Down Conversion Ratio," *IEEE Transactions on Industrial Electronics*, vol. 62, no. 8, pp. 4769-4776, 2015, https://doi.org/10.1109/TIE.2015.2397881.

[16] B. A. Ikawanty, B. Irawan, "Four-Phase Interleaved Boost Converter for Maximum Power Extraction in PV System," *Eduvest- Journal of Universal Studies*, vol. 3, no. 5, pp. 994-1006, 2023, https://doi.org/10.59188/eduvest.v3i5.818.

[17] M. Fekri, H. Farzanehfard and E. Adib, "An interleaved high step-up DC-DC converter with low input current ripple," *2016 7th Power Electronics and Drive Systems Technologies Conference (PEDSTC)*, pp. 147-152, 2016, https://doi.org/10.1109/PEDSTC.2016.7556853.

[18] G. Zhou, Q. Tian and L. Wang, "Soft-Switching High Gain Three-Port Converter Based on Coupled Inductor for Renewable Energy System Applications," *IEEE Transactions on Industrial Electronics*, vol. 69, no. 2, pp. 1521-1536, 2022, https://doi.org/10.1109/TIE.2021.3060614.

[19] O. Lopez-Santos *et al*., "Quadratic boost converter with low-output-voltage ripple," *IET power Electronics*, vol. 13, no. 8, pp. 1605–1612, 2020, https://doi.org/10.1049/iet-pel.2019.0472.

[20] P. Luo, L. Guo, J. Xu and X. Li, "Analysis and Design of a New Non-Isolated Three-Port Converter With High Voltage Gain for Renewable Energy Applications," *IEEE Access*, vol. 9, pp. 115909-115921, 2021, https://doi.org/10.1109/ACCESS.2021.3106058.

[21] T. Chaudhury and D. Kastha, "A High Gain Multiport DC–DC Converter for Integrating Energy Storage Devices to DC Microgrid," *IEEE Transactions on Power Electronics*, vol. 35, no. 10, pp. 10501-10514, 2020, https://doi.org/10.1109/TPEL.2020.2977909.

[22] M. Popuri *et al*., "Improved interleaved boost converter with soft-switching: analysis and experimental validation," *Engineering Technology & Applied Science Research*, vol. 13, no. 6, p. 12381-12389, 2023, https://doi.org/10.48084/etasr.6532.

[23] B. Akhlaghi and H. Farzanehfard, "Efficient zvt cell for interleaved dc–dc converters," *IET Power Electronics*, vol. 13, no. 10, pp. 1925-1933, 2020, https://doi.org/10.1049/iet-pel.2019.1102.

[24] A. Alzahrani, G. Devarajan, S. Subramani, V. Indragandhi, & C. Ogbuka, "Analysis and validation of multi-device interleaved dc-dc boost converter for electric vehicle applications," *IET Power Electronics*, vol. 16, no. 9, p. 1548-1557, 2023, https://doi.org/10.1049/pel2.12494.

[25] G. Calderon-Lopez, A. Villarruel-Parra, P. Kakosimos, S. Ki, R. Todd, & A. Forsyth, "Comparison of digital pwm control strategies for high-power interleaved dc–dc converters," *IET Power Electronics*, vol. 11, no. 2, p. 391-398, 2018, https://doi.org/10.1049/iet-pel.2016.0886.

[26] M. Rezvanyvardom, A. Mirzaei, & S. Rahimi, "New interleaved fully soft switched pulse width modulation boost converter with one auxiliary switch," *IET Power Electronics*, vol. 12, no. 5, p. 1053-1060, 2019, https://doi.org/10.1049/iet-pel.2018.5796.

[27] P. Thounthong, P. Mungporn, S. Pierfederici, D. Guilbert, & N. Bizon, "Adaptive control of fuel cell converter based on a new hamiltonian energy function for stabilizing the dc bus in dc microgrid applications," *Mathematics*, vol. 8, no. 11, p. 2035, 2020, https://doi.org/10.3390/math8112035.

[28] K. S. Faraj and J. F. Hussain, "Analysis and comparison of dc-dc boost converter and interleaved dc-dc boost converter," *Engineering and Technology Journal*, vol. 38, no. 5, pp. 622-635, 2020, https://doi.org/10.30684/etj.v38i5a.291.

[29] H. Akça, A. Aktas, "DC/DC boost converter topologies and experimental comparison in electric vehicle to grid applications," *Journal of Polytechnic*, 2024, https://doi.org/10.2339/politeknik.1405319.

[30] M. L. Alghaythi, R. M. O'Connell, N. E. Islam, M. M. S. Khan and J. M. Guerrero, "A High Step-Up Interleaved DC-DC Converter With Voltage Multiplier and Coupled Inductors for Renewable Energy Systems," *IEEE Access*, vol. 8, pp. 123165-123174, 2020, https://doi.org/10.1109/access.2020.3007137.

[31] S. Chen, S. Yang, C. Huang, H. Chou, & M. Shen, "Interleaved high step-up dc-dc converter based on voltage multiplier cell and voltage-stacking techniques for renewable energy applications," *Energies*, vol. 11, no. 7, p. 1632, 2018, https://doi.org/10.3390/en11071632.

[32] A. Hafez *et al*., "High power interleaved boost converter for photovoltaic applications," *Journal of Power and Energy Engineering*, vol. 6, pp. 1-17, 2018, https://doi.org/10.4236/jpee.2018.65001.

[33] A. A. M. Faudzi, S. F. Toha, R. A. Hanifah, N. F. Hasbullah, N. A. Kamisan, "An interleaved dc charging solar system for electric vehicle," *International Journal of Power Electronics and Drive Systems (IJPEDS)*, vol. 12, no. 4, p. 2414, 2021, https://doi.org/10.11591/ijpeds.v12.i4.pp2414-2422.

[34] K. -C. Tseng, C. -C. Huang and C. -A. Cheng, "A High Step-Up Converter With Voltage-Multiplier Modules for Sustainable Energy Applications," *IEEE Journal of Emerging and Selected Topics in Power Electronics*, vol. 3, no. 4, pp. 1100-1108, 2015, https://doi.org/10.1109/JESTPE.2015.2404943.

[35] M. Moradzadeh, S. Hamkari, E. Zamiri, and R. Barzegarkhoo, "Novel high step-up DC/DC converter structure using a coupled inductor with minimal voltage stress on the main switch," *Journal of Power Electronics*, vol. 16, no. 6, pp. 2005–2015, 2016, https://doi.org/10.6113/JPE.2016.16.6.2005.

[36] H. Zhu, D. Zhang, B. Zhang and Z. Zhou, "A Nonisolated Three-Port DC–DC Converter and Three-Domain Control Method for PV-Battery Power Systems," *IEEE Transactions on Industrial Electronics*, vol. 62, no. 8, pp. 4937-4947, 2015, https://doi.org/10.1109/TIE.2015.2393831.

[37] N. A. Ahmed, B. N. Alajmi, I. Abdelsalam and M. I. Marei, "Soft Switching Multiphase Interleaved Boost Converter With High Voltage Gain for EV Applications," *IEEE Access*, vol. 10, pp. 27698-27716, 2022, https://doi.org/10.1109/ACCESS.2022.3157050.

[38] J. C. Coutiño *et al*., "High Gain Boost Converter with Reduced Voltage in Capacitors for Fuel-Cells Energy Generation Systems," *Electronics*, vol. 9, no. 9, p. 1480, 2020, https://doi.org/10.3390/electronics9091480.

[39] M. Maalandish, S. H. Hosseini, S. Ghasemzadeh, E. Babaei and T. Jalilzadeh, "A Novel Multiphase High Step-Up DC/DC Boost Converter With Lower Losses on Semiconductors," *IEEE Journal of Emerging and Selected Topics in Power Electronics*, vol. 7, no. 1, pp. 541-554, 2019, https://doi.org/10.1109/JESTPE.2018.2830510.

[40] B. A. Ikawanty, M. Ashari, T. Taufik and D. Garinto, "Performance Comparison of Standard and TwoPhase DC-DC Boost Converter," *2019 International Conference on Information and Communications Technology (ICOIACT)*, pp. 800-804, 2019, https://doi.org/10.1109/ICOIACT46704.2019.8938500.

[41] B. A. Ikawanty, M. Ashari, H. Suryoatmojo and Taufik, "Low Current Ripple Control Using Particle Swarm Algorithm Based Modified Boost Converter for MPPT Application," *2021 1st International Conference on Electronic and Electrical Engineering and Intelligent System (ICE3IS)*, pp. 102-107, 2021, https://doi.org/10.1109/ICE3IS54102.2021.9649708.

[42] N. Mohan, T. M. Undeland, and W. P. Robbins, "Power Electronics: Converters, Applications, and Design," *John Wiley & Sons*, 2003, https://books.google.co.id/books/about/Power_Electronics.html?hl=pt-BR&id=oxR8vB2XjgIC&redir_esc=y.